Mon. Not. R. Astron. Soc. **000**, 1–11 (2014) Printed 15 February 2016 (MN LATEX style file v2.2)

Multi-band optical variability of three TeV Blazars on Diverse Timescales

Alok C. Gupta[1⋆], A. Agarwal[1], J. Bhagwan[1,2], A. Strigachev[3], R. Bachev[3], E. Semkov[3], H. Gaur[4], G. Damljanovic[5], O. Vince[5], Paul J. Wiita[6]

[1]*Aryabhatta Research Institute of Observational Sciences (ARIES), Manora Peak, Nainital – 263002, India*
[2]*School of Studies in Physics & Astrophysics, Pt Ravishankar Shukla University, Amanaka G.E. Road, Raipur 492010, India*
[3]*Institute of Astronomy and National Astronomical Observatory, Bulgarian Academy of Sciences, 72 Tsarigradsko Shosse Blvd., 1784 Sofia, Bulgaria*
[4]*Key Laboratory for Research in Galaxies and Cosmology, Shanghai Astronomical Observatory, Chinese Academy of Sciences, 80 Nandan Road, Shanghai 200030, China*
[5]*Astronomical Observatory, Volgina 7, 11060 Belgrade, Serbia*
[6]*Department of Physics, The College of New Jersey, 2000 Pennington Rd., Ewing, NJ 08628-0718, USA*

arXiv:1602.04200v1 [astro-ph.HE] 12 Feb 2016

Accepted ..... Received .....; in original form .....

ABSTRACT

We present our optical photometric observations of three TeV blazars, PKS 1510-089, PG 1553+113 and Mrk 501 taken using two telescopes in India, one in Bulgaria, one in Greece and one in Serbia during 2012 - 2014. These observations covered a total of 95 nights with a total of 202 B filter frames, 247 images in V band, 817 in R band while 229 images were taken in the I filter. This work is focused on multi-band flux and colour variability studies of these blazars on diverse timescales which are useful in understanding the emission mechanisms. We studied the variability characteristics of above three blazars and found all to be active over our entire observational campaigns. We also searched for any correlation between the brightness of the sources and their colour indices. During the times of variability, no significant evidence for the sources to display spectral changes correlated with magnitude was found on timescales of a few months. We briefly discuss the possible physical mechanisms most likely responsible for the observed flux variability.

Key words: galaxies: active BL Lacertae objects: general BL Lacerate objects: individual: PKS 1510-089 BL Lacerate objects: individual: PG 1553+113 BL Lacerate objects: individual: Mrk 501

1 INTRODUCTION

Flat spectrum radio quasars (FSRQs) along with BL Lacertae objects (BL Lacs) constitute the most extreme subclass of radio-loud Active Galactic Nuclei (RLAGNs) called blazars, with observed luminosity outshining their host galaxies. The dominant radiation sources in these objects are believed to originate from relativistic jets that are very strongly Doppler boosted by being viewed at angles $\lesssim 10^{\circ}$ with the observer's line of sight (LOS) (e.g. Urry & Padovani 1995). This gives rise to flux variability in all electromagnetic (EM) bands, from radio to very high energy (VHE) gamma-rays, strong optical (>3%) and radio polarization as well as superluminal motion and anisotropic radiation.

The variability of blazars may either arise from accretion disc (AD) instabilities or changes intrinsic to the relativistic jet, although interstellar scintillation can also cause observed radio variations (e.g. Heeschen et al. 1987). These fluctuations have been observed at all accessible timescales ranging from a few minutes through days and months to even decades. Blazar variability is often broadly divided into three temporal classes. Changes of few hundred to few tenths of magnitude observed in the flux of a source from minutes to less than a day are categorized as intra-day variability (IDV) or or micro-variability or intra-night variability (e.g. Kinman 1975; Wagner & Witzel 1995, Clements, Jenks, & Torres 2003; Rector & Perlman 2003; Xie et al. 2004; Gupta et al. 2008a), while variations taking place from several days to few months are usually known as short time variability (STV) and those taking from several months to many years are usually called long term variability (LTV; Gupta et al. 2004); in the latter two classes blazar variability often can exceed even 5 magnitudes.

Blazar spectral energy distributions (SEDs) consist of two different components (e.g. Mukherjee et al. 1997; Weekes 2003). At lower frequencies (radio through UV or X-rays) their energy spectrum is widely accepted to be dominated by synchrotron emission from the relativistic electrons spiraling in the magnetic field of the jets, while most X-rays and all gamma-rays are believed to be ex-

⋆ E-mail: acgupta30@gmail.com

© 2014 RAS

Table 1. Details of telescopes and instruments

Site:	A	B	C	D	E
Scale:	0.535″/pixel	0.37″/pixel	0.2825″/pixel	0.330″/pixel[a]	0.465″/pixel
Field:	$18' \times 18'$	$13' \times 13'$	$9.6' \times 9.6'$	$16.8' \times 16.8'$	15.8'x15.8'
Gain:	1.4 e^-/ADU	10 e^-/ADU	2.687 e^-/ADU	1.0 e^-/ADU	1.25 e^-/ADU
Read Out Noise:	4.1 e^- rms	5.3 e^- rms	8.14 e^- rms	8.5 e^- rms	3.75 e^- rms
Typical seeing :	1.2″to 2.0″	1″to 2.8″	1″to 2″	1.5″to 3.5″	1″to 2″

A : 1.30 meter Ritchey-Chretien Cassegrain optical telescope, ARIES, Nainital, India
B : 1.04 meter Sampuranand Telescope, ARIES, Nainital, India
C : 1.3-m Ritchey-Chretien telescope at Skinakas Observatory, University of Crete, Greece
D : 60-cm Cassegrain telescope at Astronomical Observatory Belogradchik, Bulgaria
E : 60-cm Cassegrain telescope, Astronomical Station Vidojevica - ASV
[a] With a binning factor of 1×1

plained by inverse Compton (IC) scattering of low energy photons originating from the AD or broad line region; however, in most cases the seed photons can be synchrotron photons, thus producing synchrotron self-Compton emission. Based on the location of the first peak of the SED blazars are sub-classified into low energy peaked blazars (LBLs) and high energy peaked blazars (HBLs) with first hump peaking in the NIR/optical in case of LBLs and the second one at GeV energies. In HBLs the first peak lies in UV/X-ray band and the second one at TeV $\gamma-$rays energies (e.g. Padovani & Giommi 1995; Abdo et al. 2010). According to Fossati et al. (1997), HBLs are lower luminosity objects with a higher space density and stronger magnetic fields, while LBLs are higher luminosity objects, with a lower space density possessing weaker magnetic fields. To be more quantitative, the ratio of X-ray flux in the 0.3-3.5 kev band to the radio flux density at 5 GHz, has been employed, with low-synchrotron-peaked (LSPs) objects defined as those with this ratio below $10^{-11.5}$ while for in high-synchrotron-peaked blazars (HSPs) it is greater (Padovani & Giommi 1996). Another class of blazars with SED peaks at intermediate frequencies are sometimes distinguished and are known as intermediate synchrotron peaked blazars (ISPs; Sambruna, Maraschi & Urry 1996).

Miller et al. (1989) found the first clear evidence of optical IDV. Carini (1990) found IDV in more than 80% of blazars when the duration of observations exceeded 8 hrs. Later, Gupta & Joshi (2005) studied a larger sample of AGNs and detected significant IDV in $\sim$ 10% of radio-quiet Active Galactic Nuclei (RQAGNs), 35–40% of RLAGNs (excluding blazars) when observed for $\sim$ 6 hours while IDV was seen in 80–85% of blazars when observed duration exceeded 6 hours. To understand the complex flux variation phenomenon, both quasi-continuous measurements over single nights and longer term photometric monitoring are required. Multiband variability studies help to reveal the true nature of blazars and provide valuable constraints in the emission models. From long term studies in the optical part of the EM spectra, HBLs are found to be less variable and polarized than LBLs (Jannuzi et al. 1994). They also found the amplitudes of variability to be much smaller in case of HBLs than those for LBLs. Over the past decade, many new high energy, TeV blazars have been discovered, with a recent number reaching 54 (Holder 2012; 2014), among which 80% (44 out of 54) are found to be HBLs. These TeV HBLs are characterized by strong variability on diverse timescales ranging from a few months down to even a few minutes (e.g. Begelman et al. 2008; Nalewajko et al. 2011; Gaur, Gupta, & Wiita 2012; Barkov et al. 2012). Variability studies help us to understand the particle acceleration mechanisms taking place in the relativistic jets and can shed light on the central regions of blazars, accretion processes and the structure of the jets. Rapid variability of TeV blazars at diverse timescales can be more easily observed by virtue of the high bulk Lorentz factors (often $\geqslant 25$) of the knots seen in their relativistic jets.

Table 2. Observation log of optical photometric observations of PKS 1510-089

Date of Observation (yyyy mm dd)	Telescope	Data Points (B, V, R, I)
2014 04 30	D	0,2,2,2
2014 05 20	D	0,2,2,2
2014 05 21	D	0,2,2,2
2014 05 22	D	0,2,2,2
2014 05 23	D	0,2,2,2
2014 06 15	C	3,3,3,3
2014 07 01	D	0,2,2,2
2014 07 02	D	0,2,2,2
2014 07 03	D	0,2,2,2
2014 07 04	D	0,2,2,2
2014 07 05	D	0,2,2,2
2014 07 06	C	3,3,3,3
2014 07 21	C	3,3,3,3
2014 07 22	C	3,3,3,3
2014 07 25	C	3,3,3,3
2014 07 29	C	3,3,3,3
2014 08 03	D	0,2,2,2
2014 08 18	D	0,2,2,2

The key motivation of this paper is to study flux and colour variability characteristics along with spectral changes of three TeV blazars at diverse timescales to increase our current understanding of blazar variability through photometric studies. Here we report the photometric observations of PKS 1510-089, PG 1553+113 and Mrk 501 on diverse timescales using five telescopes, starting in June 2012 and running through September 2014. This paper is organized as follows: in section 2, we describe the observations and data reduction; section 3 gives the details about the analysis techniques used; section 4 provides our results of IDV and STV/LTV along with colour variability of our sample of blazars; we present a discussion and our conclusions in section 5.

Table 3. Observation log of optical photometric observations of PG 1553+113.

Date of Observation (yyyy mm dd)	Telescope	Data Points (B, V, R, I)
2013 07 03	E	1,1,1,1
2013 07 08	E	1,1,1,1
2013 07 26	C	3,3,3,3
2013 08 28	C	3,3,3,3
2014 04 09	B	0,1,1,1
2014 04 10	B	1,1,1,1
2014 04 11	B	0,1,5,1
2014 04 22	A	2,2,33,1
2014 04 23	A	1,1,46,1
2014 05 09	B	1,1,65,1
2014 05 11	B	0,16,149,2
2014 05 17	B	1,1,67,1
2014 05 23	A	1,1,172,1
2014 05 23	D	2,2,2,2
2014 05 26	B	1,1,55,1
2014 05 27	E	3,3,3,3
2014 06 15	C	3,3,3,3
2014 07 01	D	2,2,2,2
2014 07 02	D	2,2,2,2
2014 07 03	D	2,2,2,2
2014 07 04	D	2,2,2,2
2014 07 05	D	2,2,2,2
2014 07 06	C	3,3,3,3
2014 07 21	C	3,3,3,3
2014 07 22	C	3,3,3,3
2014 07 25	C	3,3,3,3
2014 07 29	C	3,3,3,3
2014 08 18	D	2,2,2,2
2014 08 26	D	2,2,2,2

2 OBSERVATIONS AND DATA REDUCTIONS

The optical photometric observations of our blazar sample were carried out in the B, V, R, and I pass-bands, with two telescopes in India, one in Greece, one in Bulgaria and one in Serbia, all equipped with CCD detectors. The details of these five telescopes, detectors and other parameters used are given in Table 1. Over 1495 image frames covering 95 nights between June 2012 and Sept 2014 were taken for three blazars, PKS 1510-089, PG 1553+113 and Mrk 501, to study their flux and spectral characteristics on diverse timescales. Observation logs, including date of observation, number of images acquired in each filter and the telescope used are presented for the three blazars individually in Tables 2, 3 and 4.

2.1 Telescopes and Data Reduction

The optical photometric observations of these blazars were carried out using five telescopes around the world among which two telescopes are in India operated by Aryabhatta Research Institute of observational sciencES (ARIES), Nainital. One is the 1.04 m Sampuranand telescope having Ritchey-Chretien (RC) optics with a f/13 beam equipped with Johnson UBV and Cousins RI filters. The other is the 1.3-m Devasthal fast optical telescope (DFOT), which is a fast beam (f/4) telescope with a modified RC system equipped with broad band Johnson-Cousins B, V, R, I filters. DFOT provides a pointing accuracy better than 10 arcsec RMS (Sagar et al. 2011). Further details of both telescopes are given in Table 1 (telescopes A and B). We also employed the 1.3m RC telescope of Skinikas Observatory[1], of the University of Crete (Greece). Technical parameters and chip specifications for the cameras used are given in Table 1 (Telescope C). All frames were exposed through a set of standard Johnson-Cousins filters. In addition to above telescopes, we carried out photometric observations of the blazars using the 60

Table 4. Observation log of optical photometric observations of Mrk 501.

Date of Observation (yyyy mm dd)	Telescope	Data Points (B, V, R, I)
2012 06 02	C	3,3,3,3
2012 06 29	C	3,3,3,3
2012 06 30	C	3,3,3,3
2012 07 01	C	3,3,3,3
2012 07 02	C	3,3,3,3
2012 07 03	C	3,3,3,3
2012 07 04	C	3,3,3,3
2012 07 05	C	3,3,3,3
2013 07 08	E	1,1,1,1
2013 07 13	E	1,1,1,1
2013 07 14	E	1,1,1,1
2013 07 26	C	3,3,3,3
2013 08 28	C	3,3,3,3
2014 03 31	E	3,3,3,3
2014 05 22	D	0,2,2,2
2014 05 23	D	2,2,2,2
2014 05 27	E	2,3,2,3
2014 05 28	E	3,3,3,2
2014 05 28	E	5,4,5,4
2014 06 15	C	3,3,3,3
2014 06 29	E	3,3,3,3
2014 06 30	E	3,3,3,3
2014 07 01	E	3,3,3,2
2014 07 01	D	2,2,2,2
2014 07 02	D	2,2,2,2
2014 07 02	E	3,2,3,2
2014 07 03	D	2,2,2,2
2014 07 03	E	1,2,3,3
2014 07 04	D	2,2,2,2
2014 07 05	D	2,2,2,2
2014 07 05	E	2,3,3,3
2014 07 06	E	3,3,3,1
2014 07 06	C	3,3,3,3
2014 07 21	C	5,5,5,5
2014 07 22	C	5,5,5,5
2014 07 25	C	5,5,5,5
2014 07 28	C	5,5,5,5
2014 07 29	C	5,5,5,5
2014 08 02	D	2,2,2,2
2014 08 03	D	2,2,2,2
2014 08 04	D	2,2,2,2
2014 08 18	D	2,2,2,2
2014 08 19	D	2,2,2,2
2014 08 25	D	2,2,2,2
2014 08 26	D	2,2,2,2
2014 08 31	D	6,6,6,6
2014 09 18	D	2,2,2,2
2014 09 19	D	2,2,2,2

[1] Skinakas Observatory is a collaborative project of the University of Crete, the Foundation for Research and Technology – Hellas, and the Max-Planck-Institut für Extraterrestrische Physik.

cm Cassegrain telescope of Belogradchik AO, which was equipped with standard UBVRI filter sets. Instrumental details are summarized in Table 1 (Telescope D). Observations were also taken with 60cm Cassegrain telescope, which is located on Vidojevica mountain in South Serbia, through Johnson-Cousins BVRI standard filter set (Telescope E).

IRAF[2] packages were used for the pre-processing of the raw data following the steps described below. Bias frames were taken for each night at regular intervals. Taking the median of all bias frames acquired during a particular night, a master bias was generated which was subtracted from all twilight flat frames and also from the image frames taken during that night. The next step was to generate a master flat for each filter by median combining all the flat frames in a particular passband. Then each source frame is divided by normalized master flat to remove pixel to pixel inhomogenities. The final step of image pre-processing is to remove cosmic rays from all source image frames. Every science exposure was bias subtracted, dark subtracted and twilight flat fielded. Further processing was then done using the Dominion Astronomical Observatory Photometry (DAOPHOT II) software (Stetson 1987; Stetson 1992) to perform concentric circular aperture photometry and some customized scripts written in MATLAB were also used. Aperture photometry for the data obtained from telescope E, was done with MaxIm DL packages. For every night aperture photometry was carried out with four different aperture radii, i.e., $\sim 1\times$ FWHM, $2\times$ FWHM, $3\times$ FWHM and $4\times$ FWHM. Aperture radii of $2\times$ FWHM were finally adopted for our final results as they provided the best SNR. For these blazars we observed three or more comparison stars from the same field as of the source[3]. We then selected two steady comparison stars based on their proximity in magnitude and colour to the blazar.

3 VARIABILITY DETECTION CRITERION

To investigate the IDV properties of blazars we used two statistics, namely the F-test and χ^2 test which helped us to state the statistically significance of the extracted results.

3.0.1 F-Test

The F-test is considered to be a proper statistic to determine any changes of variability. F values compare two sample variances and are calculated as (e.g. Agarwal et al. 2015):

$$F_1 = \frac{Var(BL-StarA)}{Var(StarA-StarB)}, F_2 = \frac{Var(BL-StarB)}{Var(StarA-StarB)}. \quad (1)$$

Here (BL-Star A), (BL-Star B), and (Star A-Star B) are the differential instrumental magnitudes of blazar and comparison star A, blazar and comparison star B, and star A and star B, respectively, while Var(BL-Star A), Var(BL-Star B), and Var(Star A-Star B) are the variances of those differential instrumental magnitudes.

We take the average of F_1 and F_2 to find a mean observational F value. The F value is then compared with $F^{(\alpha)}_{\nu_{bl},\nu_*}$, a critical value, where ν_{bl} and ν_* respectively denote the number of degrees of freedom for the blazar and star, while α is the significance level set as 0.1 and 1 percent (i.e. 3σ and 2.6σ) for our analysis. If the mean F value is larger than the critical value, the null hypothesis (i.e., that of no variability) is discarded.

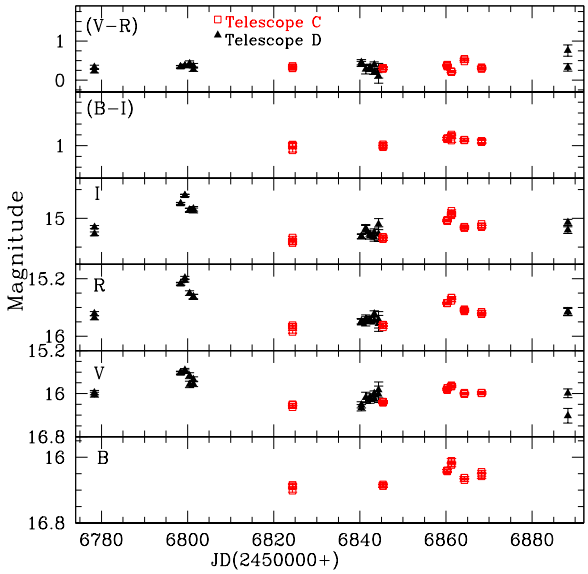

Figure 1. Short-term through long-term variability LCs and colour indices of PKS 1510−089 in the B, V, R and I bands and (B-I) and (V-R) colours. Different symbols denote data from different observatories: open red squares, telescope C; filled black triangles, telescope D.

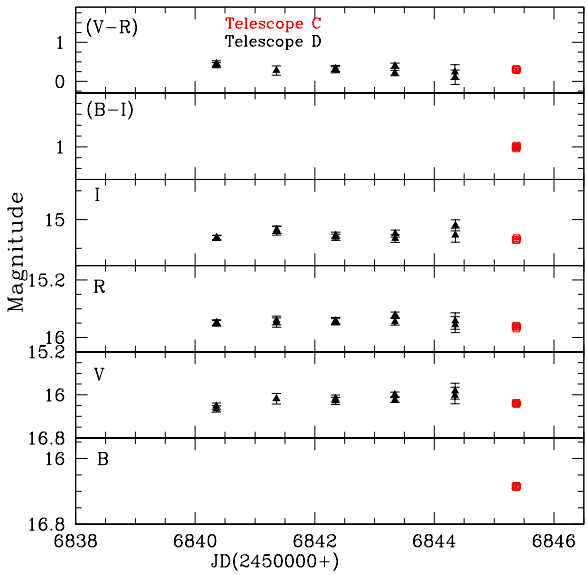

Figure 2. As in Figure 1, for the limited period around MJD 6840, providing a better view of variability in that period.

3.0.2 χ^2-test

To examine the presence or absence of IDV we also performed χ^2-test which is defined as (e.g. Agarwal & Gupta 2015):

[2] IRAF is distributed by the National Optical Astronomy Observatories, which are operated by the Association of Universities for Research in Astronomy, Inc., under cooperative agreement with the National Science Foundation.

[3] http://www.lsw.uni-heidelberg.de/projects/extragalactic/charts/

Table 5. Results of IDV observations of PG 1553+113.

Date	Band	N	F-test $F_1, F_2, F, F_c(0.99), F_c(0.999)$	χ^2test $\chi^2_1, \chi^2_2, \chi^2_{av}, \chi^2_{0.99}, \chi^2_{0.999}$	Variable	A%
22.04.2014	R	30	2.08, 1.49, 1.79, 1.20, 1.27	38.55, 26.45, 32.5, 746.39, 776.91	PV	3.0
23.04.2014	R	45	2.17, 2.63, 2.40, 1.28, 1.39	68.22, 77.19, 72.70, 413.39, 436.37	PV	1.0
09.05.2014	R	56	3.27, 3.23, 3.25, 1.89, 2.34	125.16, 103.19, 114.17, 82.29, 93.17	V	4.2
11.05.2014	R	123	1.41, 1.56, 1.49, 1.53, 1.76	98.46, 110.04, 104.25, 161.25, 176.01	NV	–
17.05.2014	R	67	1.32, 1.30, 1.31, 1.27, 1.38	48.44, 45.80, 47.12, 37.29, 460.90	PV	4.3
22.05.2014	R	170	1.08, 1.00, 1.02, 1.73, 2.08	115.87, 101.75, 108.81, 104.01, 116.09	PV	4.0
26.05.2014	R	50	2.06, 2.18, 2.12, 1.96, 2.46	75.99, 70.10, 73.04, 74.92, 85.35	PV	4.4

Var : Variable, PV : probable variable, NV : Non-Variable

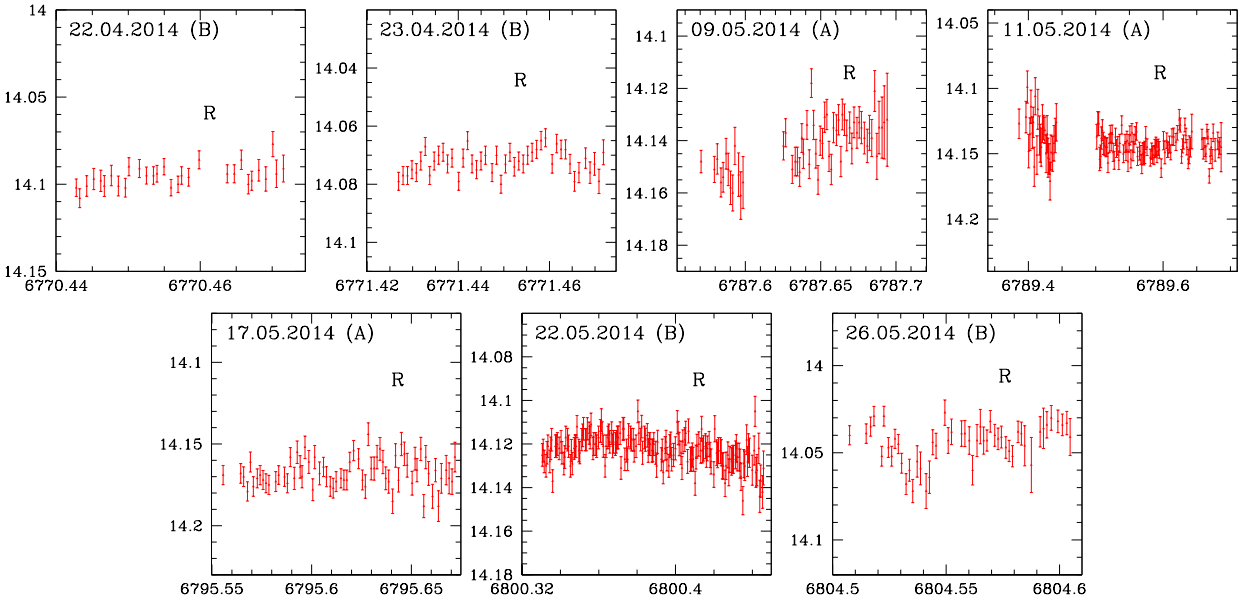

Figure 3. Light curves for PG 1553+113. In each panel, the axes are the JD (+24590000) and R-band magnitude; the observation date and the telescope used are indicated.

$$\chi^2 = \sum_{i=1}^{N} \frac{(V_i - \overline{V})^2}{\sigma_i^2}, \quad (2)$$

where, $\overline{V}$ is the mean magnitude, and the ith observation yields a magnitude V_i with a corresponding standard error σ_i, which is due to photon noise from the source and sky, CCD read-out and other non-systematic error sources. Exact quantification of such errors by the IRAF reduction package is impractical and it has been found that theoretical errors are smaller than the real errors by a factor of 1.3–1.75 (e.g., Gopal-Krishna et al. 2003) which for our data is ∼1.5, on average. So the errors obtained after data reduction should be multiplied by this factor to get better estimates of the real photometric errors. This statistic is then compared with a critical value $\chi^2_{\alpha,\nu}$ where α is again the significance level as the in case of the F-test while $\nu = N - 1$ is the number of degrees of freedom; $\chi^2 > \chi^2_{\alpha,\nu}$ implies the presence of variability.

3.0.3 Percentage amplitude variation

The percentage variation on a given night is calculated by using the variability amplitude parameter A, introduced by Heidt & Wagner (1996), and defined as

$$A = 100 \times \sqrt{(A_{max} - A_{min})^2 - 2\sigma^2}(\%). \quad (3)$$

Here, A_{max} and A_{min} are the maximum and minimum values in the calibrated LCs of the blazar, and σ is the average measurement error.

4 RESULTS

4.1 PKS 1510−089

PKS 1510−089 ($\alpha_{2000.0}$ = 15h 12m 50.53s, $\delta_{2000.0}$ = $-09^\circ05'59''$) is a FSRQ at a redshift of $z = 0.361$ (Thompson, Djorgovski, & de Carvalho 1990) and is among the highly polarized AGN. Lu (1972) first reported significant optical flux variations over a time span of ∼5 yr. During a 1948 outburst, PKS 1510–089 showed an extremely large variation of ΔB = 5.4 mag and later faded by ∼ 2.2 mag within 9 days (Liller & Liller 1975). On IDV timescales some very strong variations have been reported in optical bands: ΔR of 0.65 mag in 13 min (Xie et al. 2001) and of 2.0 mag in 42 min (Dai et al. 2001), while in V band a change of

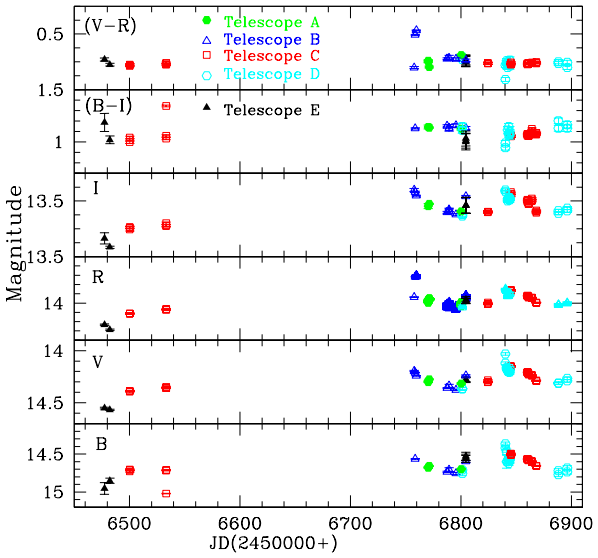

Figure 4. Long-term variability LCs and colour indices of PG 1553+113 in the B, V, R and I bands and (B-I) and (V-R) colours. Different symbols denote data from different observatories: filled green circles, telescope A; blue open triangles, telescope B; red open squares, telescope C; cyan open squares, telescope D; black closed triangles,telescope E.

1.68 mag in 60 min has been reported (Xie et al. 2002). It was detected by the EGRET instrument on-board the CGRO in the MeV-GeV energy band (Hartman et al. 1992) as γ-rays. The synchrotron emission peaks around IR frequencies and IC component seems to dominate the γ-rays . A pronounced UV bump is clearly visible in this source which can be attributed to the thermal emission from the AD around the central region (Malkan & Moore 1986; Pian & Treves 1993). A rapid γ-ray flare was reported by D'Ammando et al. (2009) in 2008 March using the AGILE satellite, while it was monitored by the Whole Earth Blazar Telescope. Later, during the high γ-ray state of this source in 2009 March, D'Ammando et al. (2011) reported detailed analysis of their multifrequency monitoring of this FSRQ using AGILE. They also found noticeable spectral variations in the near-IR through optical bands and also found thermal features in the optical/UV spectrum in the broad-band SED of this source.

4.1.1 **Flux and colour variability**

The $\sim$ 4 months LCs for the blazar PKS 1510-089 in B, V, R, and I passbands are shown in Figure 1 along with the colour indices (B-I) and (V-R). Genuine STV was present, but this source exhibited no significant colour variation during the observation span. To provide a better view of the nature of the variability of this source around MJD 6840–6846, we have plotted this same time span on an expanded scale in Figure 2.

In the following analysis, we have corrected the calibrated magnitudes for galactic extinction following the extinction map of Schlegel et al. (1998) using the NED extinction calculator[4] with values in each filter as: A_B = 0.363 mag, A_V = 0.275 mag, A_R = 0.217 mag and A_I = 0.151 mag (Cardelli et al. 1989; Bessell, Castelli, & Plez 1998). The bottom panel of Figure 1 represents

[4] `http://ned.ipac.caltech.edu`

Table 6. Results of STV/LTV studies for magnitude changes in each band.

Source	Band	Faintest Mag	JD (Min)	Brightest Mag	JD (Max)	Δm
PKS	B	16.77	2456824.4	16.41	2456861.3	0.36
1510−089	V	16.69	2456888.3	15.84	2456799.4	0.85
	R	16.16	2456824.4	15.41	2456799.4	0.75
	I	15.58	2456824.4	14.75	2456799.4	0.83
PG	B	15.21	2456533.3	14.55	2456840.4	0.66
1553+113	V	14.71	2456482.3	14.17	2456840.4	0.54
	R	14.40	2456482.3	13.81	2456759.7	0.59
	I	13.91	2456482.3	13.50	2456757.7	0.41
Mrk 501	B	15.06	2456487.4	14.65	2456806.4	0.41
	V	14.29	2456482.4	13.94	2456806.4	0.35
	R	13.90	2456482.4	13.55	2456949.3	0.35
	I	13.29	2456901.3	12.58	2456801.4	0.71

short-term/long-term variability (STV/LTV) LC of PKS 1510−089 in the B passband which includes data from 6 nights using the 1.3m RC telescope in Greece. We monitored the source in he B filter for STV/LTV studies from JD 2456824.37 to JD 2456868.27. The maximum B band magnitude attained by the source was 16.77 on JD 2456824.37 while the brightest level of B = 16.41 was reached on JD 2456861.27, which is $\sim$ 1.39 magnitude brighter than the faintest level of B = 17.8 as reported by Liller & Liller (1975), thus indicating that the source is not in a faint state and could possibly be in a post-outburst state. The corresponding STV/LTV LCs in V, R, and I passbands are displayed in the second, third and fourth panels (from the bottom) of Figure 1 using data sets from the 1.3m RC telescope in Greece and the 60 cm Cassegrain telescope in Bulgaria (telescope C & D) covering a time span between JD 2456778.37 to JD 2456888.28. The details of magnitude changes during the whole observation period are listed in Table 6 where column 1 is the source name, column 2 is the filter used for observation, Column 3 tells the faintest magnitude attained by the target and its corresponding JD is given in column 4, while the brightest value is given in column 5 , the time corresponding to it is given in column 6 and the last column gives the total magnitude range. During the entire monitoring period, the overall magnitude variations were ΔB = 0.36, ΔV = 0.85, ΔR = 0.75, and ΔI = 0.83.

The (B-I) and (V-R) colour variations as a function of JD are shown in the top two panels of Figure 1. The maximum variation in (B-I) during our observation span was found to be a modest 0.29 mag, between 1.13 mag on JD 245684.38 and 1.42 mag on JD 2456861.27 while that in (V-R) was 0.64 mag, between 0.17 mag on JD 2456844.35 and 0.81 mag on JD 2456888.28. The mean magnitudes in B, V, R, and I are 16.60, 16.25, 15.86, and 15.26 mag, respectively, while the average colour indices are (B-I) = 1.29 and (V-R) = 0.40.

4.2 PG 1553+113

PG 1553+113 ($\alpha_{2000.0}$ = 15h 55m 43.04s, $\delta_{2000.0}$ = $+11^{\circ}11^{'}24.4^{''}$) was discovered in the Palomar-Green survey of ultraviolet-excess objects as a 15.5 magnitude blue stellar object (Green, Schmidt & Liebert 1986). It is a bright optical source with R band magnitude varying from $\sim$ 13 to $\sim$ 15.5 (Miller at al. 1988) while is hads a mean V-band magnitude around 14 (Falomo & Treves 1990; Osterman et al. 2006) Due to its featureless spectra, this object was suggested to be a BL Lacertae object (Miller &

Green 1983) and its redshift determination has always been a challenge. Based on low resolution UV spectra, Miller & Green (1983) estimated its redshift $\sim$ 0.37. Based on the detection of strong Lyα + O VI absorbers, Danforth et al. (2010) proposed $z > 0.395$ while $z \leqslant 0.58$ from statistical arguments. Recently, Kapanadze (2013) found that the upper limit to its redshift should be smaller than that proposed by Danforth et al. (2010). Its classification as a HSP was determined from its SED (Falomo & Treves 1990; Donato, Sambruna, & Gliozzi 2005). Falomo et al. (1994) found its optical spectral index to be constant ($\alpha \sim$ -1) using observations between 1986 and 1991 while it underwent a variation of ΔV = 1.4. PG 1553+113 has been observed through entire EM spectra from radio through very high energy γ-rays up to 1 TeV (Aharonian et al. 2006; Albert et al. 2007b). Its log(F_{2KeV} /F_{5GHz})values range from 4.99 to 3.88, where F_{2KeV} is its 2 keV X-ray flux, while F_{5GHz} is the radio flux at 5 GHz (Osterman et al. 2006; Rector et al. 2003).

4.2.1 Flux and colour variability

We monitored PG 1553+113 in the R passband on 7 nights for a span of $\sim$ 4 hours on each night to investigate flux variability properties on intra-day timescales. The IDV plots are displayed in Figure 3 where observation date and telescope used are mentioned within the plot itself. The observation log is given in Table 3. To claim the presence or absence of intra-day variability we applied the F- and χ^2- statisitical tests, the results of which are presented in Table 5. The blazar is said to be variable (V) if the variability conditions for both tests are satisfied for the 0.999 level, while it is marked probably variable (PV) if conditions for either of the two tests are followed at the 0.99 level; while the it is marked non-variable (NV) if none of these conditions are met. We detected strong microvariability on 1 night while it was found to be PV on 5 nights and was clearly NV on only a single night.

The 1.2 year LCs in B, V, R, and I along with (B-I) and (V-R) colour variations for the blazar PKS 1553+113 are shown in Figure 4. To study optical properties on short/long timescales we investigated the target in B, V, R, and I filters observed using all 5 telescopes on 29 nights during the period between JD 2456477.5 and JD 2456896.5. We have corrected the calibrated magnitudes for galactic extinction in each filter with A_B = 0.188 mag, A_V = 0.142 mag, A_R = 0.113 mag and A_I = 0.078 mag. The details of the magnitude changes during the whole observation span for each band are listed in Table 6. Significant STV was found with moderate colour variations. The minimum R band magnitude attained by our target was of R = 13.81 on JD = 2456759.7 which is just 0.31 mag fainter than the brightest magnitude of R = 13.5 mag as observed earlier by Osterman et al. (2006), when the source was in a flaring state. So it is fair to say that we have also observed this blazar in its flaring state. During our observation time span, the overall magnitude variations were ΔB = 0.66, ΔV = 0.54, ΔR = 0.59, and ΔI = 0.41.

The values of the (B-I) and (V-R) colour indices as a function of JD are shown in top two panels of Figure 4. Plots indicate moderate colour variation. The maximum variation noticed in the source for (V-R) during the entire LC was found to be 0.35, between 0.20 mag on JD 2456840.37 and 0.55 mag on JD 2456759.70, while that in (B-I) was 1.39 between its colour range of 0.06 mag on JD 2456824.4 and 1.45 mag on JD 2456533.26. Mean magnitudes in B, V, R, and I are 14.82, 14.43, 14.07, and 13.63, while the average colour indices are (B-I) = 1.20 and (V-R) = 0.34.

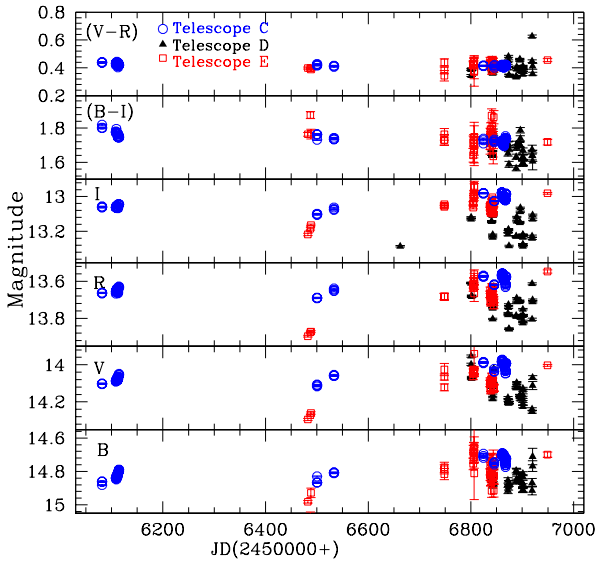

Figure 5. Long-term variability LCs and colour indices of Mrk 501 in the B, V, R and I bands and (B-I) and (V-R) colours. Different symbols denote data from different observatories: blue open circles, telescope C; black filled triangles, telescope D; and red open squares, telescope E.

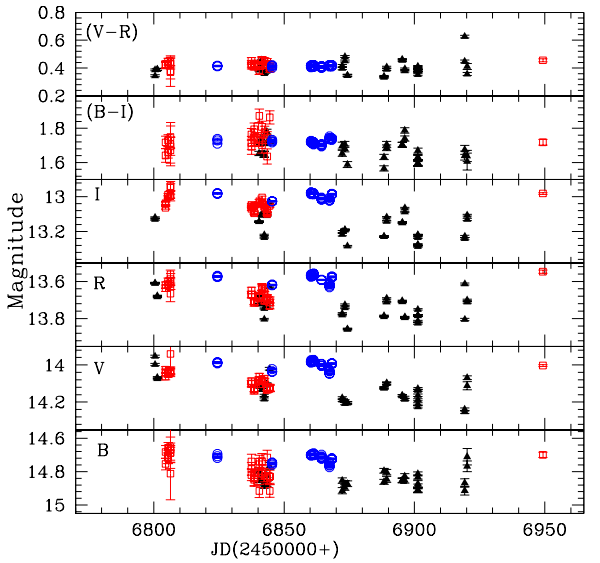

Figure 6. Data from Figure 5 expanded around MJD 6800-7000 to better show variability in that period. Symbols as in Fig. 5.

4.3 Mrk 501

Mrk 501 ($\alpha_{2000.0}$ = 16h 53m 52.13s, $\delta_{2000.0} = +39^\circ45'36.2''$) is the second closest BL Lacertae object after Mrk 421, with $z = 0.034$, and is thus an object of interest across the whole EM spectrum (Fan & Lin 1999; Kataoka et al. 1999; Sambruna 2000; Xue & Cui 2005; Gliozzi et al. 2006). The near-IR–optical spectrum of this HBL shows a strong host galaxy signature with host brightness of $\simeq$ 11.92 in R band (Nilsson et al. 2007). The SED of Mrk 501 displays a double-humped structure with peaks occurring at keV and GeV/TeV energies. The physical mechanisms responsible for

the production of GeV/TeV hump are still a topic of debate (Ghisellini & Madau 1996; Krawczynski et al. 2004; Cerruti et al. 2012). In the optical regime, Heidt & Wagner (1996) reported a flux variation of ∼32% in a time span of less than 2 weeks while Ghosh et al. (2000) reported variability in 7 out of 10 nights during March & June 1997. Mrk 501 has been found to display rapid variability on few minutes timescales over the entire EM spectra (Albert et al. 2007a; Gupta et al. 2008a), which can be attributed to relativistically beamed radiation from jets, jet deceleration (Georganopoulos & Kazanas 2003; Levinson 2007), or other plasma mechanisms (e.g. Krishan & Wiita 1994)

4.3.1 **Flux and colour variability**

The photometric magnitudes extracted during our monitoring campaign are displayed in figure 5 which shows ∼ 2.3 year LC for the blazar MRK 501. The LCs in B, V, R, and I passbands along with (B-I) and (V-R) colour variations are plotted in different panels of above figure. Figure 6 shows the nature of variability in more detail around MJD 6800-7000, when this blazar displays large variability.

The target was observed for 48 nights between 2456081.5 and 2456920.4 using five telescopes whose details are given in Table 1. Details about magnitude changes in each band during the whole monitoring period are given in Table 6. In the following analysis, we have corrected the calibrated magnitudes for galactic extinction as: A_B = 0.069 mag, A_V = 0.052 mag, A_R = 0.041 mag and A_I = 0.029 mag. The flux from the nucleus of the HBL is contaminated by the emissions of its host galaxy. So the observed magnitudes in each spectral band have also been corrected for the host galaxy contribution, following the measurements of Nilsson et al. (2007) to calculate the host galaxy contribution in R band which is then used to find the corresponding contributions for the B, V, and I bands (Fukugita et al. 1995).

During our observation time span, the overall magnitude variations were ΔB = 0.41, ΔV = 0.35, ΔR = 0.35, and ΔI = 0.71. The mean magnitudes in B, V, R, and I are 14.80, 14.09, 13.68, and 13.07, respectively. The short-term and long-term LCs of Mrk 501 in (V-R) and (B-I) colours are shown in the top two panels of Figure 5. The average colour indices are (B-I) = 1.72 and (V-R) = 0.41 The maximum variation noticed in the source for the (V-R) colour index during the entire LC was found to be 0.29 (the range was between 0.33 mag on JD 2456888.33 and 0.63 mag on JD 2456919.31), while that in (B-I) was 0.31 (this colour index ranged between 1.56 mag on JD 2456888.33 and 1.88 mag on JD 2456487.40).

4.4 Correlated variations between colour and magnitude?

As variations in the optical flux of blazars are accompanied with spectral changes, studying the colour index–magnitude relationship can be an useful tool to understand the origin of variability in blazars. In this section, we investigate the colour–magnitude relationship for all three blazars. Since spectral variations follow any optical flux variations, examining relationships between the corresponding variations in the colour indices such as (B-V), (V-R), (R-I), (B-R) or (B-I) of the three targets with respect to the variation in their brightnesses would be very helpful in understanding the variability characteristics in more detail.

Colour–magnitude (CM) plots on few months timescales for the three sources are shown in Figure 7. We have fitted straight lines (CI =mV + c) to colour index, CI against V magnitude plots for each source. The fitted values for the slope, m, and intercept

Table 7. Color–magnitude dependencies and colour-magnitude correlation coefficients on short timescales for PKS 1510-089.

Color Indices	m_1^a	c_1^a	r_1^a	p_1^a
(V-I)	0.234	−2.571	0.250	0.130
(V-R)	0.322	−5.227	0.397	0.015
(R-I)	−0.189	3.554	−0.374	0.021

[a] m_1 = slope and c_1 = intercept of CI against V;
r_1 = Pearson coefficient; p_1 = null hypothesis probability

Table 8. Color–magnitude dependencies and colour-magnitude correlation coefficients on short timescales for PG 1553+113.

Color Indices	m_1^a	c_1^a	r_1^a	p_1^a
(B-I)	0.070	0.093	0.102	0.498
(B-V)	−0.022	0.876	−0.048	0.744
(V-R)	0.114	−1.336	0.440	0.0009
(R-I)	0.012	0.660	0.054	0.704

[a] m_1 = slope and c_1 = intercept of CI against V;
r_1 = Pearson coefficient; p_1 = null hypothesis probability

c, are listed in Tables 7, 8 and 9 for PKS 1510-089, PG 1553+113 and Mrk 501, respectively, along with the linear Pearson correlation coefficients, r_1 and the corresponding null hypothesis probabilities, p_1. A positive slope here means positive correlation between the CI and the brightness of the source. Here we consider the result significant only if the null hypothesis probability is $p_1 \leqslant 0.01$ and Pearson correlation coefficient, $r \geqslant 0.5$. A significant positive correlation in these plots would physically imply that the source follows a bluer-when-brighter (BWB; or redder when fainter) trend, i.e., the source tends to be bluer when its brightness increases, while a negative slope would indicate an opposite correlation between the source magnitude and CI, indicating that the source exhibits redder-when-brighter behaviour (RWB) behaviour.

The correlation analysis results between brightness of the source and the colour indices are also given in Tables 7–9. For these sources we did not find any strong correlation (Pearson correlation coefficient, $r > 0.5$) between V band magnitude and colour indices on several months timescale.

The CM relationship at diverse timescales can help us understand the emission mechanisms responsible for blazar variability and also help pin down the emitting regions. Different CM rela-

Table 9. Color–magnitude dependencies and colour-magnitude correlation coefficients on short timescales for Mrk 501.

Color Indices	m_1^a	c_1^a	r_1^a	p_1^a
(B-I)	−0.040	2.282	−0.057	0.722
(B-V)	−0.130	3.042	−0.287	0.069
(V-R)	−0.003	0.454	−0.009	0.956
(R-I)	0.174	−1.559	0.329	0.033

[a] m_1 = slope and c_1 = intercept of CI against V;
r_1 = Pearson coefficient; p_1 = null hypothesis probability

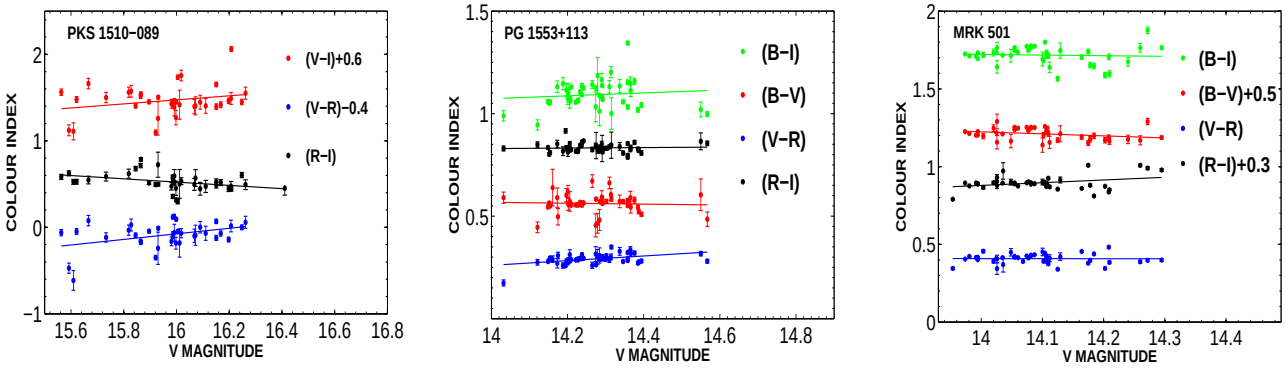

Figure 7. Colour magnitude plots on short timescales for all three blazars. The V magnitudes are given on the X-axis and the various labeled colour indices are plotted against them for each labeled source.

tionship in BL Lacs and FSRQs could be due to the existence of two varying modes, i.e., larger flux variations with lesser spectral changes or vice versa. Raiteri et al. (2003) found at most weak correlations between the source magnitude and the colour indices for the BL Lacerate object S5 0716+714, that are similar to our results. Agarwal et al. (2016) also found no evidence for the source to display spectral changes with magnitude on either of the timescales even when the BL Lac S5 0716+714 was rapidly variable. The CM relation in blazars has been found to vary among their outburst state, active state, and the faint state (Sasada et al. 2010). Optical emission from blazars is generally a combination of jet and AD radiation and usually dominated by that from the relativistic jets. However, FSRQs are usually low frequency synchrotron peaked sources, thus having a substantial contribution to the blue-UV continuum arising from thermal contamination from the AD which is expected to produce a slowly and weakly variable bluer emission component. The position of the thermal blue bump and its strength in comparison to the jet emission also affect the spectral behaviour of FSRQs. When relativistically beamed jet synchrotron emission dominates the AD emission, the BWB trend can be explained by acceleration of relativistic particles or due to injection of fresh electrons having even harder energy distribution. Sun et al. (2014) recently proposed a timescale dependent colour variation model, according to which a BWB trend in blazars is strongest for timescales of < 30 days and it eventually weakens with as timescale increases to above 100 days. Our results seem to complement this model. Densely sampled and simultaneous multiband photometric observations will be helpful in understanding the CM relationship in greater detail and in better contraining models.

5 DISCUSSION AND CONCLUSION

Blazar variability studies can help us examine the radiation mechanisms in more detail while also provide an insight on the location, size, structure, and dynamics of the emitting regions (Ciprini et al. 2003). Most mechanisms for variability in RLAGNs are expected to arise within the relativistic jet whose emission is Doppler boosted. The only significant extrinsic variability in blazars is probably seen in the radio band, where strongly frequency dependent interstellar scintillation is found to be dominant mechanism of variability at low radio frequencies. Intrinsic processes operate across all EM bands, and include directly those causing changes in the jet radio emission. Some of these clearly arise from synchrotron and Compton losses which cause electron energy losses but energy gains can come from the fresh injection of particles with energy distribution higher than that of the previous ones. Both of these processes can co-exist but operate on different timescales.

The initial origin of variability could be located in AD based fluctuations propagating into the jets, or it could start with changes in the outgoing flow, usually related to shocks in the blazar jets. According to the dominant shock-in-jet model, synchrotron and inverse Compton (IC) processes are the most common basic processes (Hughes, Aller, & Aller 2011). When those intense emitting regions are found in the highly relativistic Doppler boosted jets pointed at very small angles with respect to the LOS, variations are significantly amplified and frequency shifted owing to relativistic beaming. Changes in the jet geometry due to changing jet direction can cause variations in the bulk Doppler factor of the relativistic blobs traveling along the jet (usually in range 10-30), which in turn can lead to blazar variability at realtively long time-scales (Hovatta et al. 2009; Rani et al. 2011). The key processes responsible for blazar variability probably are due to a jet not being a stationary object which gives rise to various instabilities, turbulence (e.g. Marscher 2014; Calafut & Wiita 2015) and developing or decaying shocks. These act on a range of timescales. If δ is the the Doppler factor, since $F_\nu \propto \delta^{\sim 3}$, an increase in δ causes an increase in flux (Villata & Raiteri 1999) and also in the observed frequency ($\nu \propto \delta$). During their low states, blazar variablity can be attributed to AD instabilities since thermal emission from the central region of blazars can dominate over jet emission then. Then the variability can be explained by orbits of hot spots on the AD, including eclipsing of the hot spot by parts of the disk between the individual spot and the observer; this aspect directly depends on the geometry of the AD and also on the viewing angle of the observer. Even though optical band is a narrow part of the complete EM spectrum, it is critical in determinibg the presence of additional components other than synchrotron continuum, such as AD emission or host galaxy contribution.

The presence of both BWB and RWB trends in some blazars can be explained by superposition of both blue and red emission components where the redder one is attributed to the synchrotron radiation from the relativistic jet while the blue component could come from the thermal emission from the AD. The BWB trend may indicate that two components, one variable (with a flatter slope, α_{var}) ($f_\nu \propto \nu^{-\alpha}$) and another stable (with $\alpha_{const} > \alpha_{var}$), contribute to the overall emission in the optical regime. It also could be possibly explained with a one component synchrotron model

if the more intense the energy release, the higher the particles' frequency (Fiorucci, Ciprini, & Tosti et al. 2004). Then the BWB trend could be explained if the luminosity increase was due to injection of fresh electrons with an energy distribution harder than that of the previously cooled ones (Kirk et al. 1998; Mastichiadis & Kirk 2002). The BWB trend could also be due to Doppler factor variations in a spectrum slightly deviating from a power law (Villata et al. 2004). If optical emission is combination of emission from both jet and AD, then as the jet brightens from a low state, the colour of the combined emission gets redder as synchrotron emission from the relativistic jets is intrinsically redder than that of the AD, producing RWB behaviour. However, if even higher energy electrons are injected causing further brightening, then we get a bluer colour (BWB); this is usually dominant during an outburst state. We found a weak BWB trend, i.e., a spectrum becoming flatter when the object is brighter, in two of the sources while the opposite was found dominant in one of them.

In this paper, we have performed multiband optical photometry for three TeV blazars namely: PKS 1510−089, PG 1553+113 and Mrk 501 between 2012 and 2014 in a total of 95 nights in B, V, R, and I passbands. This allowed us to study flux and colour variability characteristics on diverse timescales. During our 7 nights of observation for IDV for PG 1553+113 we detected clear microvariability on a single night using F-statistics and χ^2-test (at 3σ significance for both). But if we include PV cases (at 2.6σ for either tests) then we can say we found the source to be variable on intraday timescales on 6 out of these 7 nights. Carini (1990) monitored about 20 blazars and found IDV in most of them. He also noticed that probability of detecting IDV increased to 80% when observed for more than 8 hours. Later, a sample of 34 BL Lacerate objects were observed by Heidt & Wagner (1996) when they found that about 75% of the sample displayed significant variations when observed for $<$ 6 hours. Carini et al. (2007) found that less than 10% of his blazar sample displayed variability on intraday timescales when observed for only $\sim$ 4-5 hours. Thus, the chances of observing IDV in blazars is greatly improved when observed for more than 6 hours. The results in this study are consistent with these earlier observations. Clearly, IDV results can be further improved by more dense and lengthier observations.

We searched for flux and colour variability on few months to few years timescales and found significant flux variations on these timescales with moderate colour variations for all three TeV blazars. We also studied the correlation between the V magnitude of the source and corresponding variations in the (B-I), (B-V), (R-I), and (V-R) colour indices. Our observations did not reveal the presence of significant correlated spectral variability in these targets on short timescales. Variability studies of larger blazar samples on minutes to years timescales are extremely important since they can provide information on numerous blazar parameters.

ACKNOWLEDGMENTS

We thank the referee for very useful comments which helped us to improve the manuscript. This research was partially supported by Scientific Research Fund of the Bulgarian Ministry of Education and Sciences under grant DO 02-137 (BIn-13/09). GD and OV gratefully acknowledge the observing grant support from the Institute of Astronomy and Rozhen National Astronomical Observatory, Bulgaria Academy of Sciences. This work is a part of the Projects No 176011 (Dynamics and kinematics of celestial bodies and systems), No. 176004 (Stellar physics) and No. 176021 (Visible and invisible matter in nearby galaxies: theory and observations) supported by the Ministry of Education, Science and Technological Development of the Republic of Serbia.

REFERENCES

Abdo A. A., et al., 2010, ApJ, 716, 30
Agarwal A., Gupta A. C., 2015, MNRAS, 450, 541
Agarwal A., et al., 2015, MNRAS, 451, 3882
Agarwal A., et al., 2016, MNRAS, 455, 680
Aharonian F., et al., 2006, A&A, 448, L43
Albert J., et al., 2007a, ApJ, 669, 1143
Albert J., et al., 2007b, ApJ, 654, L119
Barkov M. V., Aharonian F. A., Bogovalov S. V., Kelner S. R., Khangulyan D., 2012, ApJ, 749, 119
Begelman M. C., Fabian A. C., Rees M. J., 2008, MNRAS, 384, L19
Bessell M. S., Castelli F., Plez B., 1998, A&A, 333, 231
Calafut V., Wiita P. J., 2015, JApA, 36, 255
Cardelli J. A., Clayton G. C., Mathis J. S., 1989, ApJ, 345, 245
Carini M. T., 1990, PhDT,
Carini M. T., Noble J. C., Taylor R., Culler R., 2007, AJ, 133, 303
Cerruti M., Zech A., Boisson C., Inoue S., 2012, AIPC, 1505, 635
Ciprini S., Tosti G., Raiteri C. M., Villata M., Ibrahimov M. A., Nucciarelli G., Lanteri L., 2003, A&A, 400, 487
Clements S. D., Jenks A., Torres Y., 2003, AJ, 126, 37
D'Ammando F., et al., 2009, A&A, 508, 181
D'Ammando F., et al., 2011, A&A, 529, A145
Dai B. Z., Xie G. Z., Li K. H., Zhou S. B., Liu W. W., Jiang Z. J., 2001, AJ, 122, 2901
Danforth C. W., Keeney B. A., Stocke J. T., Shull J. M., Yao Y., 2010, ApJ, 720, 976
Donato D., Sambruna R. M., Gliozzi M., 2005, A&A, 433, 1163
Falomo R., Treves A., 1990, PASP, 102, 1120
Falomo R., Scarpa R., Bersanelli M., 1994, ApJS, 93, 12
Fan J. H., Lin R. G., 1999, ApJS, 121, 131
Fiorucci M., Ciprini S., Tosti G., 2004, A&A, 419, 25
Fossati G., Celotti A., Ghisellini G., Maraschi L., 1997, MNRAS, 289, 136
Fukugita M., Shimasaku K., Ichikawa T., 1995, PASP, 107, 945
Gaur H., Gupta A. C., Wiita P. J., 2012, AJ, 143, 23
Georganopoulos M., Kazanas D., 2003, ApJ, 594, L27
Ghisellini G., Madau P., 1996, MNRAS, 280, 67
Ghosh K. K., Ramsey B. D., Sadun A. C., Soundararajaperumal S., 2000, ApJS, 127, 11
Gliozzi M., Sambruna R. M., Jung I., Krawczynski H., Horan D., Tavecchio F., 2006, ApJ, 646, 61
Gopal-Krishna, Stalin C. S., Sagar R., Wiita P. J., 2003, ApJ, 586, L25
Green R. F., Schmidt M., Liebert J., 1986, ApJS, 61, 305
Gupta A. C., Banerjee D. P. K., Ashok N. M., Joshi U. C., 2004, A&A, 422, 505
Gupta A. C., Joshi U. C., 2005, A&A, 440, 855
Gupta A. C., Deng W. G., Joshi U. C., Bai J. M., Lee M. G., 2008a, NewA, 13, 375
Gupta A. C., Fan J. H., Bai J. M., Wagner S. J., 2008b, AJ, 135, 1384
Hartman R. C., et al., 1992, ApJ, 385, L1
Heeschen D. S., Krichbaum T., Schalinski C. J., Witzel A., 1987, AJ, 94, 1493
Heidt J., Wagner S. J., 1996, A&A, 305,

Holder J., 2012, APh, 39, 61
Holder J., 2014, BrJPh, 44, 450
Hovatta T., Valtaoja E., Tornikoski M., Lähteenmäki A., 2009, A&A, 494, 527
Hughes P. A., Aller M. F., Aller H. D., 2011, ApJ, 735, 81
Jannuzi B. T., Smith P. S., Elston R., 1994, ApJ, 428, 130
Kapanadze B. Z., 2013, AJ, 145, 31
Kataoka J., et al., 1999, ApJ, 514, 138
Kinman T. D., 1975, IAUS, 67, 573
Kirk R. L., et al., 1998, LPI, 29, 1752
Krishan V., Wiita P. J., 1994, ApJ, 423, 172
Krawczynski H., et al., 2004, ApJ, 601, 151
Levinson A., 2007, ApJ, 671, L29
Liller M. H., Liller W., 1975, ApJ, 199, L133
Lu P. K., 1972, AJ, 77, 829
Malkan M. A., Moore R. L., 1986, ApJ, 300, 216
Marscher A. P., 2014, ApJ, 780, 87
Mastichiadis A., Kirk J. G., 2002, PASA, 19, 138
Miller H. R., Green R. F., 1983, BAAS, 15, 957
Miller H. R., Carini M. T., Gaston B. J., Hutter D. J., 1988, ESASP, 281, 303
Miller H. R., Carini M. T., Goodrich B. D., 1989, Natur, 337, 627
Mukherjee R., et al., 1997, ApJ, 490, 116
Nalewajko K., Giannios D., Begelman M. C., Uzdensky D. A., Sikora M., 2011, MNRAS, 413, 333
Nilsson K., Pasanen M., Takalo L. O., Lindfors E., Berdyugin A., Ciprini S., Pforr J., 2007, A&A, 475, 199
Osterman M. A., et al., 2006, AJ, 132, 873
Padovani P., Giommi P., 1995, MNRAS, 277, 1477
Padovani P., Giommi P., 1996, MNRAS, 279, 526
Pian E., Treves A., 1993, ApJ, 416, 130
Raiteri C. M., et al., 2003, A&A, 402, 151
Rani B., et al., 2011, MNRAS, 417, 1881
Rector T. A., Perlman E. S., 2003, AJ, 126, 47
Rector T. A., Gabuzda D. C., Stocke J. T., 2003, AJ, 125, 1060
Sagar R., et al., 2011, CSci, 101, 1020
Sambruna R. M., Maraschi L., Urry C. M., 1996, ApJ, 463, 444
Sambruna R. M., et al., 2000, ApJ, 538, 127
Sasada M., et al., 2010, PASJ, 62, 645
Schlegel D. J., Finkbeiner D. P., Davis M., 1998, ApJ, 500, 525
Stetson P. B., 1987, PASP, 99, 191
Stetson P. B., 1992, ASPC, 25, 297
Sun Y.-H., Wang J.-X., Chen X.-Y., Zheng Z.-Y., 2014, ApJ, 792, 54
Thompson D. J., Djorgovski S., de Carvalho R., 1990, PASP, 102, 1235
Urry C. M., Padovani P., 1995, PASP, 107, 803
Villata M., Raiteri C. M., 1999, A&A, 347, 30
Villata M., et al., 2004, A&A, 421, 103
Wagner S. J., Witzel A., 1995, ARA&A, 33, 163
Weeks J. R., 2003, MPLA, 18, 2099
Xie G. Z., Li K. H., Bai J. M., Dai B. Z., Liu W. W., Zhang X., Xing S. Y., 2001, ApJ, 548, 200
Xie G. Z., Zhou S. B., Dai B. Z., Liang E. W., Li K. H., Bai J. M., Xing S. Y., Liu W. W., 2002, MNRAS, 329, 689
Xie G. Z., Zhou S. B., Li K. H., Dai H., Chen L. E., Ma L., 2004, MNRAS, 348, 831
Xue Y., Cui W., 2005, ApJ, 622, 160